European Journal of Pharmacology 863 (2019) 172678

Contents lists available at ScienceDirect

European Journal of Pharmacology

journal homepage: www.elsevier.com/locate/ejphar

Full length article

Antitumor and anti-nematode activities of α-mangostin

Joanna Markowicz[a,*], Łukasz Uram[a], Justyna Sobich[b], Laura Mangiardi[c], Piotr Maj[b], Wojciech Rode[a,b]

[a] Faculty of Chemistry, Rzeszów University of Technology, 6 Powstańców Warszawy Ave, 35-959, Rzeszów, Poland
[b] Nencki Institute of Experimental Biology, 3 Pasteur Street, 02-093, Warsaw, Poland
[c] Center for Life NanoScience, CLNS@Sapienza, Italian Institute of Technology (IIT), Viale Regina Elena 291, 00161 Rome, Italy and Dipartimento di Chimica e Tecnologie del Farmaco, Sapienza Università di Roma, Piazzale Aldo Moro 5, 00185, Rome, Italy

ARTICLE INFO

Keywords:
α-Mangostin
Glioblastoma multiforme
Squamous carcinoma
Caenorhabditis elegans
Biological activity

ABSTRACT

α-Mangostin, one of the major xanthones isolated from pericarp of mangosteen (*Garcinia mangostana* Linn), exhibits a wide range of pharmacological activities, including antioxidant, anti-inflammatory, antimicrobial as well as anticancer, both in *in vitro* and *in vivo* studies. In the present study, α-mangostin' anti-cancer and anti-parasitic properties were tested *in vitro* against three human cell lines, including squamous carcinoma (SCC-15) and glioblastoma multiforme (U-118 MG), compared to normal skin fibroblasts (BJ), and *in vivo* against *Caenorhabditis elegans*. The drug showed cytotoxic activity, manifested by decrease of cell viability, inhibition of proliferation, induction of apoptosis and reduction of adhesion at concentrations lower than 10 μM (the IC_{50} values were 6.43, 9.59 and 8.97 μM for SCC-15, U-118 MG and BJ, respectively). The toxicity, causing cell membrane disruption and mitochondria impairment, was selective against squamous carcinoma with regard to normal cells. Moreover, for the first time anti-nematode activity of α-mangostin toward *C. elegans* was described (the LC_{50} = 3.8 ± 0.5 μM), with similar effect exerted by mebendazole, a well-known anthelmintic drug.

1. Introduction

α-Mangostin belongs to the major xanthones isolated from pericarp of mangosteen (*Garcinia mangostana* L.), which has long been used in traditional medicine in South East Asia to treat inflammation, skin infection, wounds and chronic ulcer. Numerous *in vitro* and *in vivo* studies revealed α-mangostin exhibits a wide range of pharmacological activities, including antioxidant, anti-inflammatory, antimicrobial and anthelmintic (Ibrahim et al., 2016; Ovalle-Magallanes et al., 2017; Zhang et al., 2017). Since cancer treatment still remains a challenge, anticancer activity is particularly interesting and α-mangostin was demonstrated to inhibit cancer cells proliferation and metastasis, as well to induce apoptosis in certain human malignancies such as skin (Wang et al., 2011), breast (Won et al., 2014), brain (Chao et al., 2011) and digestive system (Shan et al., 2014) cancers.

α-Mangostin has been reported also to exert anticancer activity *in vivo,* with significant reduction of tumor growth through induction of apoptosis and cell cycle arrest (Zhang et al., 2017). In tongue mucoepidermoid carcinoma (YD-15) xenografts, α-mangostin increased the levels of pro-apoptotic factors (LEE et al., 2016). Mitochondria-mediated apoptosis was observed in hepatocellular carcinoma (Sk-Hep-1) xenograft mice (Hsieh et al., 2013). Cell cycle arrest induced by α-mangostin has been proven by Johnson et al. (2012) on athymic nude mice bearing prostate cancer.

Parasitic worms cause diseases mainly in developing countries with over two billions of infected (Hotez et al., 2008). Due to the relatively low number of available anthelmintics (Hu et al., 2013) and reports of increasing resistance to these drugs among human parasites (Geary, 2012; Sutherland and Leathwick, 2011), potential α-mangostin activity of this type seems also worthwhile to seek (Keiser et al., 2012). Considering several common features of cancers and parasites, as well as antiparasitic properties of certain anticancer drugs and anticancer activity of some antiparasitics (Dorosti et al., 2014; Klinkert and Heussler, 2006), potential mutual action should be taken into account. Moreover, due to an increasing necessity to reduce testing on animals, *Caenorhabditis elegans* has emerged as *in vivo* model organism for anticancer drug screening without the limitations of ethical boundaries. Importantly, 60–80% of *C. elegans* genes have human homologs and many similar conservative biological processes are described in both (Artal-Sanz et al., 2006; Kobet et al., 2014; Kyriakakis et al., 2015).

Such a wide range of biological properties of α-mangostin are related to its chemical structure (see Fig. 1). The position and the number

* Corresponding author. Faculty of Chemistry, Rzeszow University of Technology, 6 Powstańców Warszawy Ave, 35-959, Rzeszów, Poland.
E-mail address: jmarkowicz@stud.prz.edu.pl (J. Markowicz).

https://doi.org/10.1016/j.ejphar.2019.172678
Received 3 July 2019; Received in revised form 12 September 2019; Accepted 18 September 2019
Available online 19 September 2019

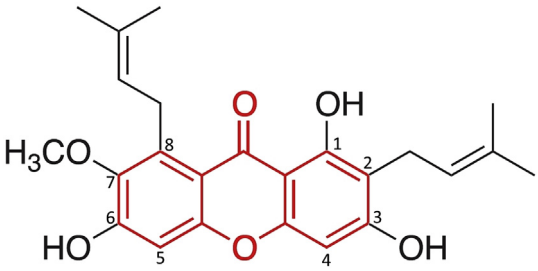

Fig. 1. Chemical structure of α-mangostin. The 9H-Xanthen-9-one ring is marked in red with a numbering of carbons.

of attached prenyl and hydroxyl groups determine its anticancer properties (Cai et al., 2016). Phenol groups on C3 and C6 are critical to anti-proliferative activity and C4 modification is capable to improve both anti-cancer and drug-like properties (Fei et al., 2014). Moreover, considering the drug's potential target, the crystal structure of α-mangostin complex (PDB 6AA4) with MTH1 hydrolase should be mentioned. MTH1 hydrolyzes oxidized nucleoside triphosphates and prevents their incorporation into DNA, making this enzyme crucial for cancer cells in oxidative stress defense and becoming a potential target for anticancer therapy (Yokoyama et al., 2019).

The present paper is aimed at assessing anti-cancer potential of α-mangostin, tested against squamous carcinoma (SCC-15) and glioblastoma multiforme (U-118 MG) cell lines, representing the most malignant and lethal types of human tumors, especially glioma (5-year survival of 5% of patients) (Ostrom et al., 2014). Studies were performed in comparison to normal fibroblasts. Cytotoxic, anti-proliferative, anti-motile and pro-apoptotic properties, as well as intracellular ATP level changes accompanying metabolic disturbances were examined. Furthermore, the drug's anti-nematode potential was checked, using *Caenorhabditis elegans* as a model of parasitic nematodes (Bürglin et al., 1998).

2. Materials and methods

2.1. Materials

α-Mangostin (purity ≥ 98% (HPLC)) was purchased from Sigma Aldrich (St Luis, MO, USA) and dissolved in dimethylsulfoxide (DMSO) to obtain 80 mM stock solution. The tested solutions of α-mangostin were prepared from stock solution in a corresponding cell culture media with adjusting the DMSO concentration to ≤0.05%, which had no significant effect on treated cells.

Human glioblastoma (U-118 MG, ATCC® HTB-15), human squamous cell carcinoma (SCC-15, ATCC® CRL-1623) and human normal fibroblast (BJ, ATCC® CRL-2522) cell lines, Dulbecco's Modified Eagle's Media (DMEM and DMEM: F-12), Eagle's Minimum Essential Medium (EMEM), fetal bovine serum (FBS), penicillin and streptomycin solution were obtained from American Type Culture Collection (ATCC, Manassas, VA, USA). Trypsin-EDTA solution, phosphate-buffered saline (PBS) with and without magnesium and calcium ions, hydrocortisone, 0.33% neutral red solution (3-amino-m-dimethylamino-2-methyl-phenazine hydrochloride), XTT sodium salt (2,3-bis[2-methoxy-4-nitro-5-sulfophenyl]-2H-tetrazolium-5-carboxanilide inner salt), phenazine-methosulfate (PMS), 0.4% trypan blue solution, dimethylsulfoxide (DMSO) and other chemicals and buffers were provided by Sigma-Aldrich (St Louis, MO, USA). DAPI (4′,6-diamidino-2-phenylindole, dihydrochloride) and CyQUANT® GR Cell Proliferation Assay Kit were purchased from Life Technologies (Carlsbad, CA, USA). CellTiter-Glo® Luminescent Cell Viability Assay for ATP level determination and Apo-ONE® Homogenous Caspase-3/7 Assay were obtained from Promega Corporation (Madison, WI, USA). All other cell culture materials were from Corning Incorporated (Corning, NY, USA), Greiner (Austria) or Nunc (Denmark).

2.2. Cell cultures

Human glioblastoma cells U-118 MG (doubling time 37 h) were cultured in DMEM, human squamous carcinoma cells SCC-15 (doubling time 48 h) were grown in DMEM: F-12 supplemented with hydrocortisone (400 ng/ml) and normal human skin fibroblasts (doubling time 1.9 day) were cultured in EMEM. All culture media contained 10% heat-inactivated FBS and 100 U/ml penicillin and 100 μg/ml streptomycin. All cell lines were cultured at 37 °C in humidified 95% air, containing 5% CO_2, with media changed every 2–3 days. Cells were passaged at 80–85% confluence after treatment with 0.25% trypsin-EDTA in PBS (calcium and magnesium ions free). Cell morphology was checked under Nikon TE2000S Inverted Microscope (Tokyo, Japan) with phase contrast. Number and viability of cells were estimated by trypan blue exclusion test using Automatic Cell Counter TC20TM (Biorad Laboratories, Hercules, CA, USA). All assays were performed in triplicates in three independent experiments.

2.3. Cytotoxicity (NR and XTT) assays

Cytotoxicity of α-mangostin was estimated by neutral red uptake (NR) and XTT reduction assays allowing determination of cellular membrane integrity and mitochondria condition, respectively. Cells were seeded in a flat, clear bottom 96-well culture plate in three replicates at a density of 1×10^4 cells/well and allowed to attach for 24 h. Then the cells were treated with α-mangostin (2.5–40 μM) for 48 h. After exposure to the drug, NR assay or XTT reduction assay was performed as earlier described (Uram et al., 2017a).

2.4. Proliferation assay

Proliferation of α-mangostin-treated cells was monitored using the CyQUANT GR Cell Proliferation Assay Kit. Cells were seeded in a flat, clear bottom 96-well plate at a density of 5×10^3 and incubated for 24 h to attach. Then the cells were treated with 5–20 μM α-mangostin solutions (200 μl/well) for 72 h, followed by centrifugation (5 min, 700 g) and gentle culture medium removal. Afterwards the plate was frozen at −80 °C and thawed (repeated twice), 200 μl/well of CyQUANT GR dye/cell-lysis buffer, prepared according to manufacturer's protocol was added, followed by incubation on a shaker for 5 min and fluorescence measurement at 480/520 nm with Tecan Infinite M200 PRO Multimode Microplate Reader (TECAN Group Ltd., Switzerland).

2.5. Cell adhesion assay

To evaluate adhesiveness of cells treated with α-mangostin, the crystal violet assay was performed. Cells were seeded in a 96-well clear plate at a density of 1×10^4 (BJ and U-118 MG) and 2×10^4 (SCC-15) cells/well, and allowed to attach for 24 h. Following attachment, cells were incubated with 5–20 μM α-mangostin solutions for 48 h, and crystal violet assay was performed as described by Uram et al. (2013).

2.6. Cell migration assay

α-Mangostin influence on cell migration was estimated using the scratch assay, known also as wound healing assay. Cells were seeded into a 24-well plate at a density of 1×10^5 (for BJ and U-118 MG) and 2×10^5 (for SCC-15) cells/well in 600 μl culture medium and incubated for 24 h to attach and reach confluence. All subsequent steps were carried out as previously described (Uram et al., 2017b). To inhibit cells proliferation and avoid false results, decrease of the FBS concentration in culture medium up to 2% was performed (Liang et al., 2007; Uram et al., 2017b). The influence of lowering FBS concentration to 2% on

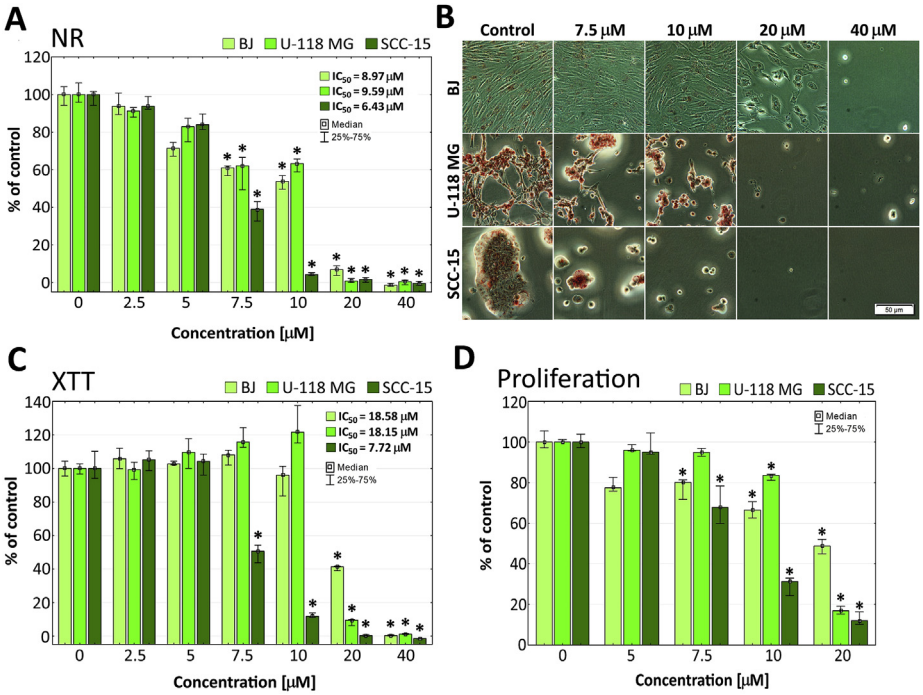

Fig. 2. Viability of BJ, U-118 MG and SCC-15 cells after 48 h treatment with α-mangostin at different concentrations, determined by neutral red uptake (A) and XTT reduction (C) assays. (D) Cancer (SCC-15 and U-118 MG) and normal (BJ) cells proliferation after 72 h incubation with α-mangostin in the range of 5–20 µM concentrations. Results, presented as medians of triplicate assays in three independent experiments, are expressed as % of non-treated controls. The whiskers are lower (25%) and upper (75%) quartile ranges. *P ≤ 0.05; Kruskal-Wallis test (against non-treated control). (B) Cell morphology and neutral red accumulation after α-mangostin treatment and 1 h incubation with neutral red dye. Red vesicles are lysosomes containing dye. Numbers indicate a micromolar concentration of α-mangostin. Images were collected with Olympus IX-83 microscope with contrast phase (scale bar = 50 µm).

cell proliferation was tested and proliferation inhibition confirmed.

2.7. Determination of intracellular ATP level

Estimation of intracellular ATP level (reflecting cell energy metabolism condition) in α-mangostin-treated cells was carried out using CellTiterGlo® Luminescent Cell assay. Cells were plated in a flat, clear bottom 96-well plates at a density of 1×10^4/well and treated with 5–20 µM α-mangostin solutions (100 µl/well) for 48 h. The CellTiter-Glo® Reagent was prepared accordingly to manufacturer's protocol and added 100 µl/well, followed by 10 min incubation on plate shaker. Luminescence was measured in Tecan Infinite M200 PRO microplate reader and adjusted relatively to the number of cells per well (the number of cells was determined by fluorescence measurement after DAPI staining).

2.8. Apoptosis assay

Apo-ONE® Homogenous Caspase-3/7 Assay was performed to verify whether α-mangostin would induce programmed cell death in tested cells. The assay allows to measure activity of caspase-3 and -7, two executive caspases involved in a late stage of apoptosis (Elmore, 2007). To perform an assay cells were seeded in a flat, clear bottom 96-well microplate (1×10^4/well) and treated with α-mangostin under conditions described above. After treatment, Apo-ONE® Caspase-3/7 Reagent was prepared according to manufacturer's protocol and added in a 1:1 vol ratio followed by 1.5 h incubation on a plate shaker. Fluorescence was read at 495/525 nm with Tecan Infinite M200 PRO Multimode Microplate Reader (TECAN Group Ltd., Switzerland), adjusted in relation to the number of cells per well (the number of cells was determined by fluorescence measurement after DAPI staining).

2.9. Toxicity to Caenorhabditis elegans, a nematode parasite model

C. elegans was maintained as previously described (Wińska et al., 2005). The effect of α-mangostin or mebendazole (the latter used as a positive control) on *C. elegans* population growth was determined according to Simpkin and Coles (1981), with the chlorhexidine pre-washing step omitted, by comparing the population levels reached in the control and test wells after 7 days of incubation at 20 °C. Tests were done in 12-well plates, with two wells used for each experimental group. Mebendazole was used in a parallel test as a positive control.

2.10. Statistical analysis

Due to the lack of normal distribution in the experimental groups, statistical analysis was performed using the non-parametric Kruskal-Wallis test to estimate the differences between the α-mangostin-treated cells and non-treated control in each cell lines, P ≤ 0.05 was considered as statistically significant. Calculations were performed using Statistica 12 (StatSoft). In addition, IC_{50} values were calculated based on results of the cytotoxicity assays (NR and XTT) using MS Excel. Medians of viability (%) were plotted against α-mangostin concentration (µM), followed by transforming the X axis to logarithmic. Using logarithmic regression, $y = a*\ln(x) + b$ equation was obtained and used to calculate the α-mangostin concentration corresponding to the cells viability decrease by 50%. The results describing reduction of *C. elegans* population are presented as LC_{50} values being means ± S.E.M., followed by the number of independent experiments (N) in parentheses.

3. Results

3.1. Cytotoxicity and cells proliferation

The biological effect of α-mangostin on normal (BJ) and cancer cells (U-118 MG and SCC-15) was estimated with two viability assays: neutral red uptake (NR) and reduction of tetrazolium salts (XTT). NR is one of the most sensitive assays, which relies on the uptake and retention of neutral red dye within lysosome compartments of the viable cells. XTT in turn, evaluates the reducing properties of *trans*-plasma membrane electron transport including the activities of mitochondrial oxidoreductases (Repetto et al., 2008; Uram et al., 2017a). Additionally, α-mangostin influence on cells proliferation after 72 h treatment was measured with the CyQUANT GR Cell Proliferation Assay Kit, which delivers CyQUANT GR dye that binds to DNA of intact cells and, after excitation at 480 nm, emits green fluorescence proportional to the cell number.

α-Mangostin revealed concentration- and cell-type-dependent

effect, in both toxicity and proliferation assays, as shown in Fig. 2.

The strongest effect of α-mangostin, monitored by the NR assay, was observed in squamous carcinoma cells, with significant decrease of their viability to about 40% at 7.5 μM concentration, then reducing it to zero at the highest concentrations. Activity of α-mangostin against U-118 MG and BJ cells was lower, with cell viability at 7.5 and 10 μM concentration being around 60%, and total viability reduction observed only at 20 and 40 μM concentrations (Fig. 2A). This effect was also visible during microscopic observations, presented in Fig. 2B. As the concentration of α-mangostin increased, accumulation of neutral red in lysosomes decreased and the cell morphology changed, followed by cells shrinkage and loss of adhesion. At 20 μM concentration only normal BJ cells were alive but at 40 μM concentration almost all cells lost their adhesion (Fig. 2B). With the use of the XTT assay similar toxicity pattern was demonstrated of α-mangostin against SCC-15 cells, with glioma and fibroblast cells showing weaker response (Fig. 2C). The highest sensitivity of SCC-15 cells to the drug, demonstrated by both NR and XTT assays, is reflected also by the IC_{50} values (insets in Fig. 2A and C).

Due to high toxicity and lack of viable cells, 40 μM concentration of α-mangostin was omitted in further studies.

The effect of α-mangostin on proliferation of investigated cells was closely correlated with its toxicity pattern (Fig. 2C). Stronger inhibition of proliferation was observed for SCC-15 cells (reduction to 12% at 7.5–20 μM drug) than glioma cells (2.5-fold weaker at 10 μM drug) or fibroblasts (reduction to 49% at 20 μM drug).

3.2. Cellular motility

Cellular motility is a cell movement from one location to another, with associated consumption of energy, constituting a very important parameter of the cancer metastasis process. Cell motility phenomenon relies on adhesion and migration of a cell, resulting from interactions of adhesion receptors on the cell surface with immobile constituents of extracellular matrix or on the surface of other cells (Soloviev et al., 2006).

Adhesion of cancer (SCC-15 and U-118 MG) and normal (BJ) cells after incubation with α-mangostin was assessed with crystal violet dye that stains DNA in the nuclei of intact adherent cells. Squamous carcinoma cells were more susceptible to the adhesion loss than glioma and fibroblast cells. Results presented in Fig. 3A, show significantly stronger decrease of adhesion of SCC-15 than fibroblasts and glioma cells under influence of α-mangostin.

At the highest concentration all tested cells lost their adhesion. Microscopic observations (Fig. 3B), in accord with results of measurement demonstrated the number of adherent cells to decrease with increasing α-mangostin concentration; in particular, this was evident for 10 μM concentration applied with SCC-15 and BJ cells.

The scratch assay is a common method for evaluation of cell migration *in vitro* (Liang et al., 2009), allowing reveal reorganization of the actin cytoskeleton and mimic to some extent migration of cells *in vivo*. In our experiments migration of cancer cells SCC-15 and U-118 MG was stopped only at 10 μM of α-mangostin, whereas migration of fibroblasts was distinctly more sensitive to the drug (decrease to the 12.7% of the control at 5 μM α-mangostin; Fig. 4A and B).

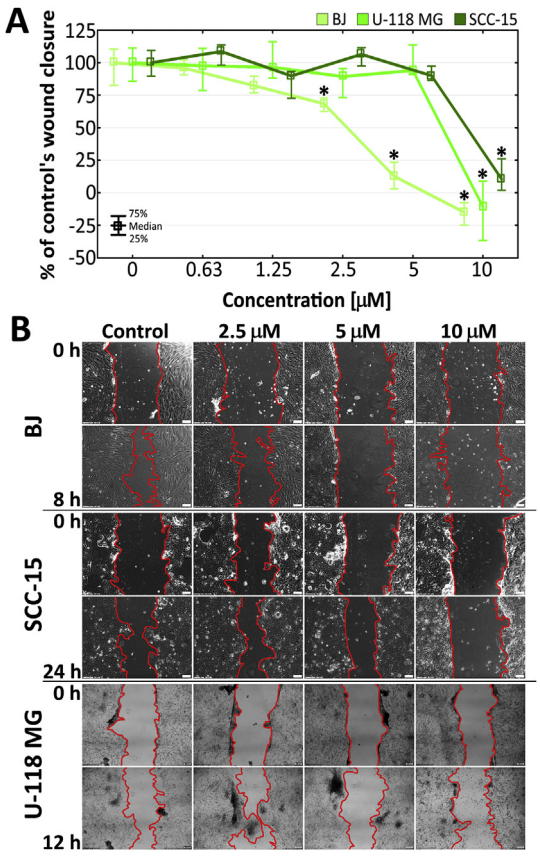

Fig. 4. (A) Cancer (SCC-15 and U-118 MG) and normal (BJ) cells migration after incubation with α-mangostin at the range of 0.63–10 μM concentrations estimated with scratch assay. Results are presented as medians and whiskers are lower (25%) and upper (75%) quartile ranges. *P ≤ 0.05, Kruskal-Wallis test (against non-treated control). (B) Representative images of scratch assay of BJ, SCC-15 and U-118 MG cells treated with α-mangostin. Images were obtained using inverted phase contrast microscope (10 × objective for BJ and SCC-15, scale bar = 100 μm; 4 × objective for U-118 MG, scale bar = 200 μm).

3.3. Apoptosis and ATP level changes

In order to determine pro-apoptotic activity of α-mangostin and its influence on intracellular ATP level in the studied cells, the Apo-ONE® Homogenous Caspase-3/7 (Promega) and CellTiterGlo® Luminescent Cell (Promega) assays were applied. The results are shown as a

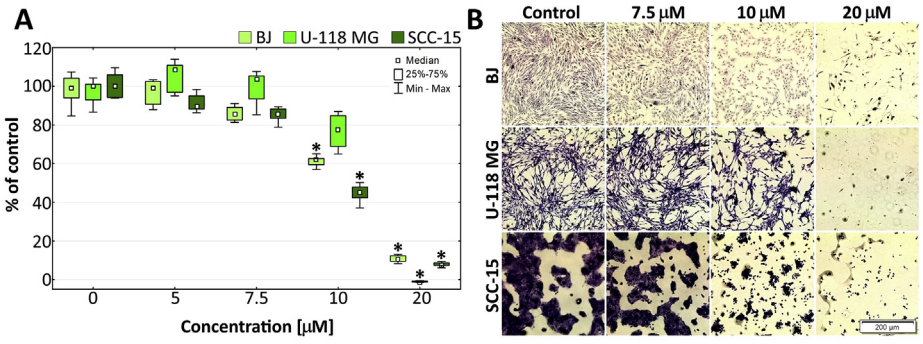

Fig. 3. Adhesiveness of BJ, U-118 MG and SCC-15 cells after 48 h incubation with α-mangostin at different concentrations obtained with crystal violet assay. A) Results are medians of triplicate assays of three independent experiments expressed as a % of non-treated controls. The whiskers are lower (25%) and upper (75%) quartile ranges. *P ≤ 0.05, Kruskal-Wallis test (against non-treated control). B) Cells morphology and adhesion to the bottom of 96-well plate after 48 h α-mangostin treatment and after 30 min incubation with crystal violet. Numbers indicate a micromolar concentration of α-mangostin. Images collected with Olympus IX-83 microscope with contrast phase. Violet signal: crystal violet, scale bar = 200 μm.

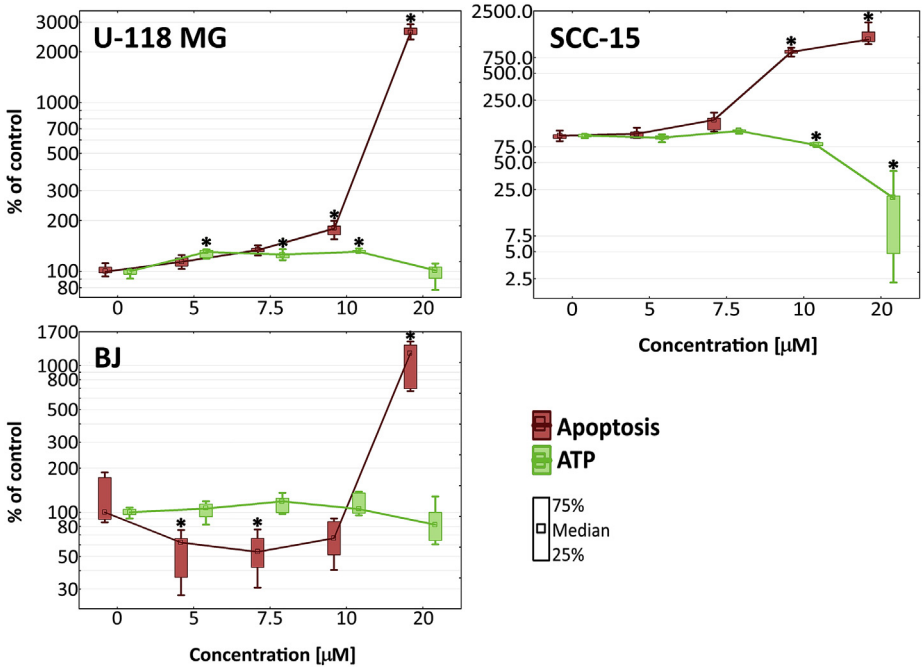

Fig. 5. Changes of caspase-3/7 activity and intracellular ATP level in BJ, U-118 MG and SCC-15 cells after 48 h treatment with 5–20 μM concentration range of α-mangostin, measured with Apo-ONE® Homogenous Caspase-3/7 assay and CellTiterGlo® Luminescent Cell assay, respectively. Results are medians of triplicate assays from three independent experiments expressed as a % of non-treated controls and presented in logarithmic graph. The whiskers are lower (25%) and upper (75%) quartile ranges. *P ≤ 0.05, Kruskal-Wallis test (against non-treated control).

relationship between the intracellular ATP level and executioner caspases activity in each cell line (Fig. 5).

α-Mangostin induced apoptosis in all the tested cell lines, with lower concentrations affecting cancer than normal cells. While a significant increase of caspases activity in SCC-15 and U-118 MG cells was apparent already at 10 μM α-mangostin, the corresponding effect in fibroblasts required 20 μM of drug. At 10 μM α-mangostin caspase-3/7 activity in squamous carcinoma cells was 5-fold higher than in glioma cells (865% and 180% of control, respectively). Interestingly, in fibroblasts at non-toxic concentrations a significant decrease of caspse-3/7 activity was observed.

When activity of caspases in SCC-15 cells has been raising, intracellular ATP level was undergoing reduction to 80%, and then to 12%. Different effect was seen in U-118 MG cells, where at the non-toxic concentrations of the drug, activity of caspases was not growing but ATP level significantly increased to 130% and then returned to control level at the highest drug concentration. In case of fibroblasts, no changes in the intracellular ATP level were observed at the range of studied concentrations.

3.4. Toxicity to C. elegans

The nematode *Caenorhabditis elegans*, a multicellular organism widely recognized as a model for basic biological and medical research, is also used to model a live animal in anti-cancer drug screening (Kobet et al., 2014). In the present study it was used to model parasitic nematodes, in order to test a potential antiparasitic effect of α-mangostin. The results revealed α-mangostin to cause reduction of growth of *C. elegans* population with the LC_{50} value of 3.8 ± 0.5 μM (5). Of note is that mebendazole, tested in parallel experiments, showed slightly lower activity, reflected by the LC_{50} value of 4.0 ± 0.5 μM (10), the latter in accord with the finding of 1.2 μM concentration of this drug being the minimum detectable dose against *C. elegans* (Simpkin and Coles, 1981).

4. Discussion

α-Mangostin shows strong pharmacological effects in a variety cancer models, including breast, prostate, lung, colon, pancreatic cancer and leukemia, both *in vitro* and *in vivo* (Akao et al., 2008; Cai et al., 2016; Ibrahim et al., 2016). Cai et al. (2016) revealed that α-mangostin inhibits cell proliferation in four hepatocellular carcinoma (HCC) cell lines in a dose- and time-dependent manner, with the IC_{50} values in the range of 10 μM, by inducing the G0/G1 phase cell cycle arrest. Anti-proliferative effect of α-mangostin was demonstrated also by Matsumoto et al. (2005) with human colon cancer cells (DLD-1), where the drug caused cell-cycle arrest in the G1 phase and subsequent induction of apoptosis *via* the intrinsic pathway resulting in nuclear condensation and fragmentation. The same author described studies on four human leukemia cell lines (HL60, K562, NB4 and U937) and reported cell growth inhibition and apoptosis induction at 5–10 μM concentrations of α-mangostin after 24–72 h incubation (Matsumoto et al., 2003).

The presented results are in line with reports from other researchers. The strongest cytotoxic effect was seen in squamous carcinoma cells with the IC_{50} equal 6.43 μM (NR assay) and total viability reduction at concentrations ≥ 10 μM after 48 h treatment. The toxic effect of α-mangostin in SCC-15 cells caused the disruption of the cell membrane integrity and mitochondria functions. Similar toxic effect against human skin cancer cells was observed for human oral squamous carcinoma cells (HSC-2, HSC-3 and HSC-4 cell lines). The IC_{50} values determined after 24 h treatment were 8–10 μM (Kwak et al., 2016) and for human melanoma cell lines, SK-MEL-2 and SK-MEL-30 after 48 h of incubation with α-mangostin, the IC_{50} values were 8.14 μM and 7.78 μM, respectively (Xia et al., 2016). Likewise, for human melanoma cells SK-MEL-28, the IC_{50}, determined after 48 h treatment, was 5.92 μM (Wang et al., 2011). Also Kaomongkolgit et al. (2011) found that α-mangostin at 3 μg mL^{-1}(7.32 μM) concentration after 48 h exposure, displayed moderate cytotoxicity against head and neck squamous carcinoma cell lines (HN-22, HN-30, and HN-31 cells) with inhibition rates of 45%–60%.

Glioma and fibroblast cells showed a weaker response in both tests, as confirmed by the IC_{50} values, which in the XTT assay for U-118 MG were 2-fold higher than for SCC-15 cells (18.15 μM against 7.72 μM), and a significant decrease of cell viability was seen at concentrations above 20 μM. Moreover, α-mangostin-mediated-toxicity in glioma and fibroblasts was mostly achieved by destroying cell membrane. Stronger effect of α-mangostin against two glioblastoma cell lines has been revealed by Chao et al. (2011), who obtained the IC_{50} values 6.4 μM for GBM8401 and 7.3 μM for DBTRG-05MG after 48 h treatment using WST-1 assay.

Anticancer activity of α-mangostin was also manifested by inhibition of cell proliferation. After 72 h treatment with α-mangostin, SCC-15 cells displayed significant reduction of proliferation at concentrations ≥7.5 μM. However, U-118 MG cells showed a lower sensitivity than SCC-15 (83% against 31% at 10 μM), with BJ cells exhibiting the weakest response.

Cytotoxic effect of α-mangostin also affected cells motility. This parameter was assessed by crystal violet and scratch assay, which determine cells adhesion and migration, respectively. Cell adhesion plays an essential role in stimulating signals that regulate cell differentiation, cell cycle, cell migration and cell survival. Dysregulation of these cellular processes is involved in initiation and/or progression of various diseases including cancer metastasis. The cell adhesion plays a pivotal role in the driving force production of the cell migration (Zhong et al., 2012). Cell adhesiveness is generally reduced in human cancers and decreases in line with their increasing "metastatic potential". Tumor cells are characterized by changes in adhesion to ECM (extracellular matrix) due to possessed alterations in the expression and pattern of plasma-membrane protein complexes (Ahmad Khalili and Ahmad, 2015; Uram et al., 2017b).

Some research groups have studied anti-metastatic potential of α-mangostin. In the research conducted by Zhang et al. (2018) α-mangostin inhibited migration of A549 cells in a dose-dependent manner. At 5 μM concentration, cellular migration was found to be inhibited by almost 33% and in the presence of 10 μM α-mangostin, migration was inhibited by 60%. It has been proven that α-mangostin displayed anti-metastatic effects also in human skin cancer cell lines, melanoma and squamous cell carcinoma. Beninati et al. (2014) observed a marked reduction (by 70%) of the adhesion of human melanoma cells (A375) and the invasion decrease by 38% and 28% in SK-MEL-28 and A375 cells, respectively after treatment with 15 μM α-mangostin. According to Wang et al. (2012), α-mangostin inhibited motility, adhesion, migration and invasion of human squamous carcinoma (A-431) and human melanoma (SK-MEL-28) cells after 48-h treatment. The migration inhibitory effect was found to be concentration-dependent and was the most marked for the concentration of 1.25 μg/ml (3.05 μM) for A-431 (migration reduced to 6%) and 2.5 μg/ml (6.1 μM) for SK-MEL-28 (migration reduced to 23%). The adhesive capability decreased to around 55% and to 61% for A-431 and SK-MEL-28 cells, respectively.

In our research, α-mangostin showed the strongest effect of reducing cellular adhesion in squamous carcinoma cells. This cell line demonstrated 60% loss of adhesion at 10 μM concentration of α-mangostin while glioma cells did not reveal significant adhesion decrease at the same concentration. Moreover, at toxic α-mangostin concentrations, migration of each tested cell line was reduced to about zero, however at non-toxic concentrations (< 10 μM) ability to migrate was affected only in normal cells. Referring to cytotoxicity results, at 10 and 20 μM concentrations of α-mangostin, all tested cells remained dead, so the adhesion and migration decrease is likely due to the toxic action of the compound, therefore it will not have the anti-metastatic potential. Such effect would be suspected if the reduction of cancer cells adhesion and/or migration occurred at non-toxic concentrations.

α-Mangostin potential to induce apoptosis has been documented by numerous studies. Zhang et al. (2018) demonstrated that drug treatment caused a dose-dependent induction of apoptosis, associated by an increased Bax/Bcl-2 ratio in human lung cancer cell (A549). According to Wang et al. (2011), α-mangostin induced apoptosis in human melanoma SK-MEL-28 cell line, due to caspase activation and mitochondrial membrane pathway disruption, revealed by 25-fold increase in caspase-3 activity and 9-fold decrease in mitochondrial membrane potential when compared to untreated cells. In accord, α-mangostin induced mitochondrial-dependent apoptosis in human hepatoma SK-Hep-1 cells (Hsieh et al., 2013), and in human leukemia HL60 cells (Matsumoto et al., 2004), with activation of caspase-9 and -3 but not caspase-8. Parameters of mitochondrial dysfunctions such as swelling, loss of membrane potential, decrease in intracellular ATP, ROS accumulation and cytochrome *c*/AIF release, were observed within 1 or 2 h after the treatment, indicating that α-mangostin preferentially targets mitochondria in the early phase. There is also an evidence of Chao et al. (2011) that α-mangostin in 2.5–10 μM concentrations does not induce apoptotic cell death in glioblastoma cells (GBM8401 and DBTRG-05MG cell lines) after 48 h of incubation, but autophagy with formation of acidic vesicular organelles (AVOs) and autophagic vacuoles.

In our research, α-mangostin induced apoptosis both in cancer and normal cells, but in squamous carcinoma cells this process has started earlier, with caspase 3 and 7 activities 5-fold higher than in glioblastoma cells. In addition, induction of apoptosis in SCC-15 cells was accompanied by ATP decrease. Pradelli et al. (2014) established the loss of energy production during apoptosis, orchestrated by caspases, to be involved in the dismantling of the dying cell. Interestingly, U-118 MG cells at non-toxic concentrations of α-mangostin displayed increase of ATP level, presumably providing energy for pro-apoptotic proteins synthesis. In contrast, fibroblasts showed no changes of ATP level in the drug-treated cells. In this context it should be mentioned that Pradelli et al. (2014) demonstrated the decrease of cellular ATP level during apoptosis in a caspase-dependent manner, as a consequence of a caspase-dependent inhibition of glycolysis.

Certain selectivity of α-mangostin, showing stronger toxicity toward tumor squamous carcinoma than glioblastoma and normal cells, according with previous observations of cell type-dependent drug activity and related potential for human skin cancer and leukemia treatment (Kaomongkolgit et al., 2011; Matsumoto et al., 2003). Moreover, it is noteworthy that α-mangostin preferentially targeted cancer cells over non-cancerous cells, indicating some potential as a chemopreventive or selective anticancer agent (Shan et al., 2011).

Of particular interest is anti-nematode activity of α-mangostin, especially as the drug is similarly toxic toward *C. elegans* as mebendazole, a known anthelmintic drug (McKellar and Scott, 1990; Simpkin and Coles, 1981), and rather more toxic than certain other anthelmintics, including albendazole (Hu et al., 2013; Sant'anna et al., 2013), ivermectin, nitazoxanide and pyrantel (Hu et al., 2013). Of note is also that α-mangostin lacked activity or showed only low activity against several other nematode species (Keiser et al., 2012). Thus, further parallel studies of antiparasitic and anticancer properties of α-mangostin and its analogues are warranted, aimed at potential shared target (s) (Dorosti et al., 2014).

5. Conclusions

α-Mangostin, a xanthone derivative from the pericarp of the mangosteen, with a wide range of biological activity (Ibrahim et al., 2016), displayed at concentrations lower than 10 μM cytotoxic activity, manifested by cell viability decrease, inhibition of proliferation, induction of apoptosis and reduction of adhesion. The toxicity, causing cell membrane disruption and mitochondria impairment, showed certain selectivity, being somewhat stronger with tumor squamous carcinoma than glioblastoma and normal cells. Of interest, α-mangostin demonstrates, beside antitumor also anti-nematode activity, suggesting further studies in search of mechanism(s) of both activities.

CRediT author statement

Joanna Markowicz: Conceptualization, Methodology, Formal Analysis, Investigation, Writing-Original Draft, Writing-Review & Editing, Visualization, Project Administration

Łukasz Uram: Methodology, Formal Analysis, Investigation, Resources, Writing-Review & Editing

Justyna Sobich: Methodology, Formal Analysis, Investigation

Laura Mangiardi: Conceptualization

Piotr Maj: Methodology

Wojciech Rode: Conceptualization, Resources, Writing-Original

Draft, Writing-Review & Editing

Acknowledgments

This work was supported by grants 2014/13/D/NZ3/02825 and 2016/21/B/NZ1/00288 from the National Science Centre, Poland. Stimulating discussions and cooperation from COST Action CM1407 are acknowledged.

References

Ahmad Khalili, A., Ahmad, M.R., 2015. A review of cell adhesion studies for biomedical and biological applications. Int. J. Mol. Sci. 16, 18149–18184. https://doi.org/10.3390/ijms160818149.

Akao, Y., Nakagawa, Y., Iinuma, M., Nozawa, Y., 2008. Anti-cancer effects of xanthones from pericarps of mangosteen. Int. J. Mol. Sci. 9, 355–370.

Artal-Sanz, M., de Jong, L., Tavernarakis, N., 2006. Caenorhabditis elegans: a versatile platform for drug discovery. Biotechnol. J. 1, 1405–1418. https://doi.org/10.1002/biot.200600176.

Beninati, S., Oliverio, S., Cordella, M., Rossi, S., Senatore, C., Liguori, I., Lentini, A., Piredda, L., Tabolacci, C., 2014. Inhibition of cell proliferation, migration and invasion of B16-F10 melanoma cells by α-mangostin. Biochem. Biophys. Res. Commun. 450, 1512–1517. https://doi.org/10.1016/j.bbrc.2014.07.031.

Bürglin, T.R., Lobos, E., Blaxter, M.L., 1998. Caenorhabditis elegans as a model for parasitic nematodes. Int. J. Parasitol. 28, 395–411.

Cai, N., Xie, S.-J., Qiu, D.-B., Jia, C.-C., Du, C., Liu, W., Chen, J.-J., Zhang, Q., 2016. Potential effects of α-mangostin in the prevention and treatment of hepatocellular carcinoma. J. Funct. Foods 26, 309–318. https://doi.org/10.1016/j.jff.2016.08.014.

Chao, A.-C., Hsu, Y.-L., Liu, C.-K., Kuo, P.-L., 2011. α-Mangostin, a dietary xanthone, induces autophagic cell death by activating the AMP-activated protein kinase pathway in glioblastoma cells. J. Agric. Food Chem. 59, 2086–2096. https://doi.org/10.1021/jf1042757.

Dorosti, Z., Yousefi, M., Sharafi, S.M., Darani, H.Y., 2014. Mutual action of anticancer and antiparasitic drugs: are there any shared targets? Future Oncol. 10, 2529–2539. https://doi.org/10.2217/fon.14.65.

Elmore, S., 2007. Apoptosis: a review of programmed cell death. Toxicol. Pathol. 35, 495–516. https://doi.org/10.1080/01926230701320337.

Fei, X., Jo, M., Lee, B., Han, S.-B., Lee, K., Jung, J.-K., Seo, S.-Y., Kwak, Y.-S., 2014. Synthesis of xanthone derivatives based on α-mangostin and their biological evaluation for anti-cancer agents. Bioorg. Med. Chem. Lett 24, 2062–2065. https://doi.org/10.1016/j.bmcl.2014.03.047.

Geary, T.G., 2012. Are new anthelmintics needed to eliminate human helminthiases? Curr. Opin. Infect. Dis. 25, 709–717. https://doi.org/10.1097/QCO.0b013e328359f04a.

Hotez, P.J., Brindley, P.J., Bethony, J.M., King, C.H., Pearce, E.J., Jacobson, J., 2008. Helminth infections: the great neglected tropical diseases. J. Clin. Investig. 118, 1311–1321. https://doi.org/10.1172/JCI34261.

Hsieh, S.-C., Huang, M.-H., Cheng, C.-W., Hung, J.-H., Yang, S.-F., Hsieh, Y.-H., 2013. α-Mangostin induces mitochondrial dependent apoptosis in human hepatoma SK-Hep-1 cells through inhibition of p38 MAPK pathway. Apoptosis 18, 1548–1560. https://doi.org/10.1007/s10495-013-0888-5.

Hu, Y., Ellis, B.L., Yiu, Y.Y., Miller, M.M., Urban, J.F., Shi, L.Z., Aroian, R.V., 2013. An extensive comparison of the effect of anthelmintic classes on diverse nematodes. PLoS One 8, e70702. https://doi.org/10.1371/journal.pone.0070702.

Ibrahim, M.Y., Hashim, N.M., Mariod, A.A., Mohan, S., Abdulla, M.A., Abdelwahab, S.I., Arbab, I.A., 2016. α-Mangostin from Garcinia mangostana Linn: an updated review of its pharmacological properties. Arabian J. Chem. 9, 317–329. https://doi.org/10.1016/j.arabjc.2014.02.011.

Johnson, J.J., Petiwala, S.M., Syed, D.N., Rasmussen, J.T., Adhami, V.M., Siddiqui, I.A., Kohl, A.M., Mukhtar, H., 2012. α-Mangostin, a xanthone from mangosteen fruit, promotes cell cycle arrest in prostate cancer and decreases xenograft tumor growth. Carcinogenesis 33, 413–419. https://doi.org/10.1093/carcin/bgr291.

Kaomongkolgit, R., Chaisomboon, N., Pavasant, P., 2011. Apoptotic effect of alpha-mangostin on head and neck squamous carcinoma cells. Arch. Oral Biol. 56, 483–490. https://doi.org/10.1016/j.archoralbio.2010.10.023.

Keiser, J., Vargas, M., Winter, R., 2012. Anthelminthic properties of mangostin and mangostin diacetate. Parasitol. Int. 61, 369–371. https://doi.org/10.1016/j.parint.2012.01.004.

Klinkert, M.Q., Heussler, V., 2006. The use of anticancer drugs in antiparasitic chemotherapy. Mini Rev. Med. Chem. 6, 131–143. https://doi.org/10.2174/138955706775475939.

Kobet, R.A., Pan, X., Zhang, B., Pak, S.C., Asch, A.S., Lee, M.-H., 2014. Caenorhabditis elegans: a model system for anti-cancer drug discovery and therapeutic target identification. Biomol Ther (Seoul) 22, 371–383. https://doi.org/10.4062/biomolther.2014.084.

Kwak, H.-H., Kim, I.-R., Kim, H.-J., Park, B.-S., Yu, S.-B., 2016. α -mangostin induces apoptosis and cell cycle arrest in oral squamous cell carcinoma cell. Evid. Based Complement Altern. Med. 2016 1–10. https://doi.org/10.1155/2016/5352412.

Kyriakakis, E., Markaki, M., Tavernarakis, N., 2015. Caenorhabditis elegans as a model for cancer research. Mol. Cell. Oncol. 2, e975027. https://doi.org/10.4161/23723556.2014.975027.

LEE, H.N., JANG, H.Y., KIM, H.J., SHIN, S.A., CHOO, G.S., PARK, Y.S., KIM, S.K., JUNG, J.Y., 2016. Antitumor and apoptosis-inducing effects of α-mangostin extracted from the pericarp of the mangosteen fruit (Garcinia mangostana L.) in YD-15 tongue mucoepidermoid carcinoma cells. Int. J. Mol. Med. 37, 939–948. https://doi.org/10.3892/ijmm.2016.2517.

Liang, C.-C., Park, A.Y., Guan, J.-L., 2007. *In vitro* scratch assay: a convenient and inexpensive method for analysis of cell migration *in vitro*. Nat. Protoc. 2, 329–333. https://doi.org/10.1038/nprot.2007.30.

Liang, M., Yang, H., Fu, J., 2009. Nimesulide inhibits IFN-gamma-induced programmed death-1-ligand 1 surface expression in breast cancer cells by COX-2 and PGE2 independent mechanisms. Cancer Lett. 276, 47–52. https://doi.org/10.1016/j.canlet.2008.10.028.

Matsumoto, K., Akao, Y., Kobayashi, E., Ohguchi, K., Ito, T., Tanaka, T., Iinuma, M., Nozawa, Y., 2003. Induction of apoptosis by xanthones from mangosteen in human leukemia cell lines. J. Nat. Prod. 66, 1124–1127. https://doi.org/10.1021/np020546u.

Matsumoto, K., Akao, Y., Ohguchi, K., Ito, T., Tanaka, T., Iinuma, M., Nozawa, Y., 2005. Xanthones induce cell-cycle arrest and apoptosis in human colon cancer DLD-1 cells. Bioorg. Med. Chem. 13, 6064–6069. https://doi.org/10.1016/j.bmc.2005.06.065.

Matsumoto, K., Akao, Y., Yi, H., Ohguchi, K., Ito, T., Tanaka, T., Kobayashi, E., Iinuma, M., Nozawa, Y., 2004. Preferential target is mitochondria in alpha-mangostin-induced apoptosis in human leukemia HL60 cells. Bioorg. Med. Chem. 12, 5799–5806. https://doi.org/10.1016/j.bmc.2004.08.034.

McKellar, Q.A., Scott, E.W., 1990. The benzimidazole anthelmintic agents–a review. J. Vet. Pharmacol. Ther. 13, 223–247.

Ostrom, Q.T., Bauchet, L., Davis, F.G., Deltour, I., Fisher, J.L., Langer, C.E., Pekmezci, M., Schwartzbaum, J.A., Turner, M.C., Walsh, K.M., Wrensch, M.R., Barnholtz-Sloan, J.S., 2014. The epidemiology of glioma in adults: a "state of the science" review. Neuro Oncol. 16, 896–913. https://doi.org/10.1093/neuonc/nou087.

Ovalle-Magallanes, B., Eugenio-Pérez, D., Pedraza-Chaverri, J., 2017. Medicinal properties of mangosteen (Garcinia mangostana L.): a comprehensive update. Food Chem. Toxicol. 109, 102–122. https://doi.org/10.1016/j.fct.2017.08.021.

Pradelli, L.A., Villa, E., Zunino, B., Marchetti, S., Ricci, J.-E., 2014. Glucose metabolism is inhibited by caspases upon the induction of apoptosis. Cell Death Dis. 5, e1406. https://doi.org/10.1038/cddis.2014.371.

Repetto, G., del Peso, A., Zurita, J.L., 2008. Neutral red uptake assay for the estimation of cell viability/cytotoxicity. Nat. Protoc. 3, 1125–1131. https://doi.org/10.1038/nprot.2008.75.

Sant'anna, V., Vommaro, R.C., de Souza, W., 2013. Caenorhabditis elegans as a model for the screening of anthelminthic compounds: ultrastructural study of the effects of albendazole. Exp. Parasitol. 135, 1–8. https://doi.org/10.1016/j.exppara.2013.05.011.

Shan, T., Cui, X., Li, W., Lin, W., Lu, H., Li, Y., Chen, X., Wu, T., 2014. α-Mangostin suppresses human gastric adenocarcinoma cells in vitro via blockade of Stat3 signaling pathway. Acta Pharmacol. Sin. 35, 1065–1073. https://doi.org/10.1038/aps.2014.43.

Shan, T., Ma, Q., Guo, K., Liu, J., Li, W., Wang, F., Wu, E., 2011. Xanthones from mangosteen extracts as natural chemopreventive agents: potential anticancer drugs. Curr. Mol. Med. 11, 666–677.

Simpkin, K.G., Coles, G.C., 1981. The use of Caenorhabditis elegans for anthelmintic screening. J. Chem. Technol. Biotechnol. 31, 66–69. https://doi.org/10.1002/jctb.503310110.

Soloviev, D.A., Pluskota, E., Plow, E.F., 2006. Cell adhesion and migration assays. Methods Mol. Med. 129, 267–278. https://doi.org/10.1385/1-59745-213-0:267.

Sutherland, I.A., Leathwick, D.M., 2011. Anthelmintic resistance in nematode parasites of cattle: a global issue? Trends Parasitol. 27, 176–181. https://doi.org/10.1016/j.pt.2010.11.008.

Uram, Ł., Szuster, M., Filipowicz, A., Zaręba, M., Wałajtys-Rode, E., Wołowiec, S., 2017a. Cellular uptake of glucoheptoamidated poly(amidoamine) PAMAM G3 dendrimer with amide-conjugated biotin, a potential carrier of anticancer drugs. Bioorg. Med. Chem. 25, 706–713. https://doi.org/10.1016/j.bmc.2016.11.047.

Uram, Ł., Szuster, M., Gargasz, K., Filipowicz, A., Wałajtys-Rode, E., Wołowiec, S., 2013. In vitro cytotoxicity of the ternary PAMAM G3-pyridoxal-biotin bioconjugate. Int. J. Nanomed. 8, 4707–4720. https://doi.org/10.2147/IJN.S53254.

Uram, Ł., Szuster, M., Misiorek, M., Filipowicz, A., Wołowiec, S., Wałajtys-Rode, E., 2017b. The effect of G3 PAMAM dendrimer conjugated with B-group vitamins on cell morphology, motility and ATP level in normal and cancer cells. Eur. J. Pharm. Sci. 102, 275–283. https://doi.org/10.1016/j.ejps.2017.03.022.

Wang, J.J., Sanderson, B.J.S., Zhang, W., 2012. Significant anti-invasive activities of α-mangostin from the mangosteen pericarp on two human skin cancer cell lines. Anticancer Res. 32, 3805–3816.

Wang, J.J., Sanderson, B.J.S., Zhang, W., 2011. Cytotoxic effect of xanthones from pericarp of the tropical fruit mangosteen (Garcinia mangostana Linn.) on human melanoma cells. Food Chem. Toxicol. 49, 2385–2391. https://doi.org/10.1016/j.fct.2011.06.051.

Wińska, P., Gołos, B., Cieśla, J., Zieliński, Z., Fraczyk, T., Wałajtys-Rode, E., Rode, W., 2005. Developmental arrest in Caenorhabditis elegans dauer larvae causes high expression of enzymes involved in thymidylate biosynthesis, similar to that found in Trichinella muscle larvae. Parasitology 131, 247–254.

Won, Y.-S., Lee, J.-H., Kwon, S.-J., Kim, J.-Y., Park, K.-H., Lee, M.-K., Seo, K.-I., 2014. α-Mangostin-induced apoptosis is mediated by estrogen receptor α in human breast cancer cells. Food Chem. Toxicol. 66, 158–165. https://doi.org/10.1016/j.fct.2014.01.040.

Xia, Y., Li, Y., Westover, K.D., Sun, J., Chen, H., Zhang, J., Fisher, D.E., 2016. Inhibition of cell proliferation in an NRAS mutant melanoma cell line by combining sorafenib and α-mangostin. PLoS One 11, e0155217. https://doi.org/10.1371/journal.pone.0155217.

Yokoyama, T., Kitakami, R., Mizuguchi, M., 2019. Discovery of a new class of MTH1 inhibitor by X-ray crystallographic screening. Eur. J. Med. Chem. 167, 153–160. https://doi.org/10.1016/j.ejmech.2019.02.011.

Zhang, C., Yu, G., Shen, Y., 2018. The naturally occurring xanthone α-mangostin induces ROS-mediated cytotoxicity in non-small scale lung cancer cells. Saudi J. Biol. Sci. 25, 1090–1095. https://doi.org/10.1016/j.sjbs.2017.03.005.

Zhang, K., Gu, Q., Yang, K., Ming, X., Wang, J., 2017. Anticarcinogenic effects of α-mangostin: a review. Planta Med. 83, 188–202. https://doi.org/10.1055/s-0042-119651.

Zhong, Y., He, S., Ji, B., 2012. Mechanics in mechanosensitivity of cell adhesion and its roles in cell migration. Int. J. Comput. Mater. Sci. Eng. 1, 1250032. https://doi.org/10.1142/S2047684112500327.